

Infrared image blurring with distance beyond an initial aperture plane

J.A. Grzesik^a

Allwave Corporation, 3860 Del Amo Boulevard, Suite 404 Torrance, CA 90503, USA

Received: 24 March 2019 / Revised: 4 July 2019

Published online: 17 October 2019

© The Author(s) 2019. This article is published with open access at Springerlink.com

Abstract. A photon field, be it in the visible or the infrared, necessarily diverges with distance away from its source. In the domain of visible optics such divergence is routinely countered through the intervention of focusing lenses or mirrors. Such focusing, on the other hand, is less readily available in the infrared, and it becomes of some interest to acquire an intuitive, semi-quantitative feel for the image blurring which this divergence implies. The present short note, whose content, admittedly, is both highly idealized and is aimed at a merely methodological goal, seeks to provide just such an image blurring insight. It considers as its datum a circular aperture with an isotropic radiant flux incident upon it, and then tracks image spreading and the concomitant intensity decline across downstream capture planes. The anticipated blurring so confirmed should encourage similar, more incisive analyses in realistic imaging scenarios. And, while the language below exudes an aura of urgency in a specifically infrared domain, its concern implicitly extends to photonic fields at all other frequencies.

1 Objective

Infrared (IR) detection clearly can depend upon measurement solely of the intensity, with all hope bypassed of any reference to phase. Indeed, IR sources must be deemed as *a priori* incoherent, and in any event the frequencies involved (on the order of 10^{15} Hz (see footnote¹)) seem to lie prohibitively beyond the measurement reach of existing microwave equipment. The question then arises as to the utility of IR intensity (IRI) collection across any given datum plane. In particular, given the spatial IRI resolution upon some ideally positioned aperture plane, what is the prognosis as to its resolution both upstream and downstream in the IR signal ray field?

The outlook, alas, is not altogether favorable. This is because, at the enormous frequencies involved, IR propagation adheres less to a Maxwell-type, wave picture than it does to a diffusive one, based as it is on a ray field governed by a simplified, Boltzmann-type transport equation. An automatic consequence of that equation is to mandate a blurring of IRI planar resolution along the downstream direction, even if, on the contrary, improvement may be expected on approach to the IR source. It is our hope that the developments indicated below will serve to substantiate some of these features.

2 Infrared signal propagation past an ideally situated aperture plane

We consider the IR field to be described by a steady-state intensity flux $\psi(\mathbf{r}, \boldsymbol{\Omega})$ (units of watt cm^{-2}) which varies together with spatial position \mathbf{r} and photon flight direction $\boldsymbol{\Omega}$. We neglect scattering², but do retain an option for

^a e-mail: jan.grzesik@hotmail.com

¹ A near-IR photon field having a wavelength of 1 micron (μm) vibrates at a frequency of roughly 3×10^{14} Hz. Phase measurement prospects appear little improved even at the deep-IR wavelength of $10 \mu\text{m}$, the operating regime of the powerful CO_2 laser. By way of temperature calibration *vis-à-vis* Wien's displacement law in the context of blackbody thermal radiation, a $1 \mu\text{m}$ wavelength corresponds to a temperature of roughly 2900 K whereas a Wien peak at $10 \mu\text{m}$ emanates from a 290 K object ten times cooler.

² Allowance for scattering, even when that latter is restricted to be isotropic in the observation frame, injects enormous complications into both phenomenology and its subjacent mathematics.

spatial attenuation as provided by a non-vanishing macroscopic absorption cross-section Σ_a (see footnote³). Under these restrictions the Boltzmann equation, essentially nothing more than a statement of IR photon bookkeeping, reads

$$\boldsymbol{\Omega} \cdot \nabla \psi(\mathbf{r}, \boldsymbol{\Omega}) + \Sigma_a \psi(\mathbf{r}, \boldsymbol{\Omega}) = 0. \quad (1)$$

We assume that we capture some information regarding $\psi(\mathbf{r}, \boldsymbol{\Omega})$ across a sensor plane having an axial coordinate $z = 0$ (displacements transverse to this axis are tagged by vector $\boldsymbol{\rho} = \{x, y\}$)⁴, which is to say that, while we can of course presume to measure, along any plane having a fixed z , only the net axial intensity flux

$$P(\boldsymbol{\rho}, z) = \int_{(2\pi)} \cos \vartheta \psi(\boldsymbol{\rho}, z, \boldsymbol{\Omega}) d\boldsymbol{\Omega}, \quad (2)$$

we will speak in what follows as if we did indeed have access to $\psi(\boldsymbol{\rho}, 0, \boldsymbol{\Omega})$ itself⁵.

With these preliminaries disposed of, we easily infer on the basis of (1) that the radiant flux $\psi(\boldsymbol{\rho}, z, \boldsymbol{\Omega})$, at any downstream station having $z > 0$, reads

$$\psi(\boldsymbol{\rho}, z, \boldsymbol{\Omega}) = e^{-z \Sigma_a \sec \vartheta} \psi(x - z \tan \vartheta \cos \varphi, y - z \tan \vartheta \sin \varphi, 0, \boldsymbol{\Omega}), \quad (3)$$

with flux $\psi(x - z \tan \vartheta \cos \varphi, y - z \tan \vartheta \sin \varphi, 0, \boldsymbol{\Omega})$ on the right-hand side being that which exists on the datum plane with $z = 0$, but having its transverse arguments suitably adjusted so as to track photon movement along direction $\boldsymbol{\Omega}$ (see footnote⁶).

3 A simple example: Isotropic disk image on aperture plane $z = 0$

By way of a simple illustration we consider the IR image on the aperture plane $z = 0$ to be isotropic within a disk of radius R (see footnote⁷). Thus

$$\psi(\boldsymbol{\rho}, 0, \boldsymbol{\Omega}) = \begin{cases} 1/2\pi & ; \quad \{\rho < R\} \cap \{\Omega_z > 0\} \\ 0 & ; \quad \{\rho > R\} \cup \{\Omega_z < 0\}, \end{cases} \quad (4)$$

³ Σ_a *per se* is built up as a product $\Sigma_a = N\sigma_a$ of the spatial atom density N and the microscopic absorption cross section σ_a . Σ_a evidently is gauged in units of cm^{-1} .

⁴ In what follows we parametrize the photon flight direction in terms of spherical angles $\{\vartheta, \varphi\}$, reckoned, respectively, from axes z and x . With axial coordinate z retained then as an explicit label, it remains only to parametrize transverse vector $\boldsymbol{\rho}$, and this is done by setting $\boldsymbol{\rho} = \rho\{\cos \phi, \sin \phi\}$, angle ϕ being measured counterclockwise from axis x toward axis y .

⁵ Since the source of IR radiation is assumed here to lie to the left of the aperture plane, and to have thus a negative axial coordinate $z < 0$, $\psi(\boldsymbol{\rho}, 0, \boldsymbol{\Omega})$ necessarily vanishes for all retrograde photon flight directions with $\vartheta > \pi/2$. On the other hand, since *all* surrounding objects themselves figure as IR sources, a statement as to such directional selectivity can only be understood modulo some agreement as to how high one should set the IR noise threshold.

⁶ The right-hand side of (3) is readily seen to recapture its prescribed boundary value when $z \downarrow 0+$. It is most easily gotten by subjecting (1) to Fourier transformation *vis-à-vis* transverse coordinate $\boldsymbol{\rho}$, *viz.*,

$$\tilde{\psi}(\boldsymbol{\kappa}, z, \boldsymbol{\Omega}) = \int_{-\infty}^{\infty} e^{-i\boldsymbol{\kappa} \cdot \boldsymbol{\rho}} \psi(\boldsymbol{\rho}, z, \boldsymbol{\Omega}) d\boldsymbol{\rho},$$

whereupon (1) is reduced to the ordinary differential equation

$$\frac{d\tilde{\psi}(\boldsymbol{\kappa}, z, \boldsymbol{\Omega})}{dz} + \left\{ \frac{i\boldsymbol{\kappa} \cdot \boldsymbol{\Omega} + \Sigma_a}{\Omega_z} \right\} \tilde{\psi}(\boldsymbol{\kappa}, z, \boldsymbol{\Omega}) = 0,$$

the Fourier inversion

$$\psi(\boldsymbol{\rho}, z, \boldsymbol{\Omega}) = \frac{1}{4\pi^2} \int_{-\infty}^{\infty} e^{i\boldsymbol{\kappa} \cdot \boldsymbol{\rho}} \tilde{\psi}(\boldsymbol{\kappa}, z, \boldsymbol{\Omega}) d\kappa_x d\kappa_y$$

of whose solution

$$\tilde{\psi}(\boldsymbol{\kappa}, z, \boldsymbol{\Omega}) = e^{-z\{i\boldsymbol{\kappa} \cdot \boldsymbol{\Omega} + \Sigma_a\}/\Omega_z} \tilde{\psi}(\boldsymbol{\kappa}, 0, \boldsymbol{\Omega})$$

immediately results in (3) once reference is also made to the angular parametrization of flight vector $\boldsymbol{\Omega}$.

There is of course no *a priori* impediment to entertaining solution (3) even *upstream* of the aperture plane, with $z < 0$, certainly all the way down to a first encounter with the IR source *per se*. However, we will regard the upstream, $z < 0$ domain as forbidden and inaccessible, and simply let it go at that.

⁷ The analysis about to ensue, and the numerical calculation which it supports, will confirm that this aperture image is indeed optimal, by reason of its minimal spread, as compared to any possible images downstream.

with a corresponding intensity flux

$$P(\rho, 0) = \frac{1}{2\pi} \int_{(2\pi)} \cos \vartheta \sin \vartheta \, d\vartheta \, d\varphi = \frac{1}{2}; \quad \{\rho < R\} \tag{5}$$

and a total energy transfer in the amount $\pi R^2/2$.

In the context of (3) we become limited thus, on any downstream image plane, to the spatial/directional domain

$$\{\rho^2 + z^2 \tan^2 \vartheta - 2\rho z \tan \vartheta \cos(\varphi - \phi) < R^2\} \cap \{\Omega_z > 0\} \tag{6}$$

which, when stated in the form

$$z^2 \tan^2 \vartheta - 2\rho z \tan \vartheta \cos(\varphi - \phi) + \rho^2 - R^2 < 0, \tag{7}$$

leads one to consider the quadratic equation in $\tan \vartheta$

$$z^2 \tan^2 \vartheta - 2\rho z \tan \vartheta \cos(\varphi - \phi) + \rho^2 - R^2 = 0 \tag{8}$$

with roots

$$\tan \vartheta_{\pm} = \frac{\rho \cos(\varphi - \phi) \pm \sqrt{\rho^2 \cos^2(\varphi - \phi) + R^2 - \rho^2}}{z}. \tag{9}$$

Since (7), *qua* function of $\tan \vartheta$, is concave up, the operational meaning of these roots is that they limit the range available to $\tan \vartheta$ in accordance with

$$\max\{0, \tan \vartheta_{-}\} < \tan \vartheta < \tan \vartheta_{+}. \tag{10}$$

For $\rho < R$ this translates into

$$0 < \tan \vartheta < \tan \vartheta_{+}, \tag{11}$$

without any additional restriction on photon flight azimuth φ , whereas, for $\rho > R$, the corresponding statement reads

$$\tan \vartheta_{-} < \tan \vartheta < \tan \vartheta_{+}, \tag{12}$$

but now with the added caveat that

$$|\varphi - \phi| < \sin^{-1}(R/\rho). \tag{13}$$

Equations (11)–(13) are easily motivated on geometrical grounds with the aid of some rudimentary sketches, best undertaken in private and without any further comment at this point⁸.

Accordingly, we now find

$$P(\rho, z) = \frac{1}{\pi} \int_{\phi}^{\phi+\pi} d\varphi \int_0^{\vartheta_{+}} e^{-z \Sigma_a \sec \vartheta} \cos \vartheta \sin \vartheta \, d\vartheta \tag{14}$$

for $\rho < R$, and

$$P(\rho, z) = \frac{1}{\pi} \int_{\phi}^{\phi+\sin^{-1}(R/\rho)} d\varphi \int_{\vartheta_{-}}^{\vartheta_{+}} e^{-z \Sigma_a \sec \vartheta} \cos \vartheta \sin \vartheta \, d\vartheta \tag{15}$$

if instead $\rho > R$. Both forms (14) and (15) are of course insensitive to spatial azimuth ϕ , a fact emphasized in their more explicit versions

$$P(\rho, z) = \frac{1}{\pi} \int_0^{\pi} d\varphi \int_0^{\vartheta_{+}} e^{-z \Sigma_a \sec \vartheta} \cos \vartheta \sin \vartheta \, d\vartheta \tag{16}$$

for $\rho < R$, and

$$P(\rho, z) = \frac{1}{\pi} \int_0^{\sin^{-1}(R/\rho)} d\varphi \int_{\vartheta_{-}}^{\vartheta_{+}} e^{-z \Sigma_a \sec \vartheta} \cos \vartheta \sin \vartheta \, d\vartheta \tag{17}$$

if instead $\rho > R$. Polar quadrature limits ϑ_{\pm} in (14) and (15) continue to make reference to spatial azimuth ϕ , and thus abide by the content of (9) in its native form. In (16) and (17), by contrast, all reference to ϕ has vanished, with ϑ_{\pm} suitably replaced by

$$\vartheta_{\pm} = \tan^{-1} \left\{ \frac{\rho \cos \varphi \pm \sqrt{\rho^2 \cos^2 \varphi + R^2 - \rho^2}}{z} \right\}. \tag{18}$$

⁸ Equation (13), in particular, should be greeted with a sigh of relief, inasmuch as it protects the square root in (9) from manufacturing unwanted imaginaries whenever $\rho > R$. And, of course, from a general perspective, it is gratifying indeed that (9), gotten here via a purely algebraic route on the basis of (7) and (8), should succeed in capturing the geometric attributes of mildly intricate ray configurations.

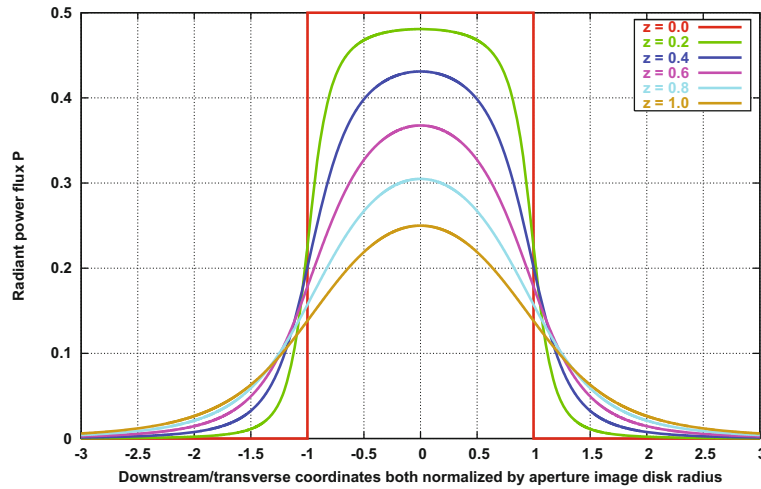


Fig. 1. Radiant power flux profile broadening with height z above aperture plane. Uniform, isotropic flux across a disk in the aperture plane at $z = 0$. Input power flux $P = 1/2$.

In the most favorable situation with $\Sigma_a = 0$ we find that structures (14)–(17) all devolve into single quadratures, first as

$$P(\rho, z) = \frac{1}{2\pi} \int_{\phi}^{\phi+\pi} \sin^2 \vartheta_+ d\varphi \tag{19}$$

for $\rho < R$, and

$$P(\rho, z) = \frac{1}{2\pi} \int_{\phi}^{\phi+\sin^{-1}(R/\rho)} \{ \sin^2 \vartheta_+ - \sin^2 \vartheta_- \} d\varphi \tag{20}$$

if instead $\rho > R$, and then, with their azimuthal invariance against ϕ fully acknowledged, as

$$P(\rho, z) = \frac{1}{2\pi} \int_0^{\pi} \frac{(\rho \cos \varphi + \sqrt{\rho^2 \cos^2 \varphi + R^2 - \rho^2})^2}{z^2 + (\rho \cos \varphi + \sqrt{\rho^2 \cos^2 \varphi + R^2 - \rho^2})^2} d\varphi \tag{21}$$

for $\rho < R$, and

$$P(\rho, z) = \frac{1}{2\pi} \int_0^{\sin^{-1}(R/\rho)} \left[\frac{(\rho \cos \varphi + \sqrt{\rho^2 \cos^2 \varphi + R^2 - \rho^2})^2}{z^2 + (\rho \cos \varphi + \sqrt{\rho^2 \cos^2 \varphi + R^2 - \rho^2})^2} - \frac{(\rho \cos \varphi - \sqrt{\rho^2 \cos^2 \varphi + R^2 - \rho^2})^2}{z^2 + (\rho \cos \varphi - \sqrt{\rho^2 \cos^2 \varphi + R^2 - \rho^2})^2} \right] d\varphi \tag{22}$$

otherwise. Here the definition dichotomy for ϑ_{\pm} persists as before, with (21)–(22) enjoying the benefit of streamlined version (18), whereas (19)–(20) remain bound to its two-variable precursor (9).

4 Sample calculation

There seems to be little possibility of carrying out in analytic terms the quadratures spelled out in eqs. (21) and (22) and, *a fortiori*, those in (16) and (17)⁹. Outright numerical treatment seems to be the only recourse, a goal achieved in code transcription, with a sample of its output summarized in fig. 1. This plot, in particular, abides by an *a priori* demand that (16) should blend smoothly into (17) and (21) into (22) as ρ sweeps past R . Code output confirms moreover that the composite profile provided by (21) and (22) does in fact respect, to an adequate approximation, the power normalization

$$\int_0^{\infty} \rho P(\rho, z) d\rho = R^2/4 \tag{23}$$

vis-à-vis (5).

⁹ Even the mighty MATHEMATICA is brought to its knees when invoked against (21)–(22).

5 A comment on the meager state of the photon streaming literature

The available infrared literature is noticeably silent on the issue of pure photon streaming. On the other hand, discussions that are close in spirit can be found in neutron transport theory [1,2]. Quite understandably, and in marked contrast to our present scenario of a planar aperture, they give pride of place to neutron streaming that originates on spherical shells.

Publisher's Note The EPJ Publishers remain neutral with regard to jurisdictional claims in published maps and institutional affiliations.

Open Access This is an open access article distributed under the terms of the Creative Commons Attribution License (<http://creativecommons.org/licenses/by/4.0>), which permits unrestricted use, distribution, and reproduction in any medium, provided the original work is properly cited.

References

1. K.M. Case, F. de Hoffmann, G. Placzek, *Introduction to the Theory of Neutron Diffusion*, Vol. 1 (Los Alamos Scientific Laboratory, Los Alamos, NM, 1953) pp. 3–12.
2. Kenneth M. Case, Paul F. Zweifel, *Linear Transport Theory* (Addison-Wesley Publishing Company, Reading, MA, 1967) pp. 35–37.